Cellular/Molecular

A Novel RNA-Binding Protein in Neuronal RNA Granules: Regulatory Machinery for Local Translation

Nobuyuki Shiina,[1,2,3] **Kazumi Shinkura,**[1] **and Makio Tokunaga**[1,2,4]

[1]Structural Biology Center, National Institute of Genetics, and [2]Department of Genetics, School of Life Science, The Graduate University for Advanced Studies, Mishima, Shizuoka 411-8540, Japan, [3]Tsukita Cell Axis Project, Exploratory Research for Advanced Technology, Japan Science and Technology Corporation, Kyoto 600-8813, Japan, and [4]Research Center for Allergy and Immunology, RIKEN, Yokohama, Kanagawa 230-0045, Japan

Local translation in neuronal dendrites is an important basis for long-term synaptic plasticity, and RNA granules in the dendrites are involved in the local translation. Here, we identify RNG105 (RNA granule protein 105), a novel RNA-binding protein, as a component of the RNA granules in dendrites of hippocampal neurons. The RNG105-localizing RNA granules contain mRNAs, the translational products of which play key roles in synaptic plasticity. RNG105 has an ability to repress translation both *in vitro* and *in vivo*, consistent with the finding that the RNA granule is translationally arrested in the basal conditions. Dissociation of RNG105 from the RNA granules is induced by BDNF, a growth factor responsible for synaptic plasticity. The RNG105 dissociation is coincident with the induction of local translation near the granules. These findings suggest that RNG105 is a translational repressor in the RNA granules and provide insight into the link between RNG105 dynamics and local translational regulation.

Key words: **translation; dendrites; RNA granules; RNG105; BDNF; synaptic plasticity**

Introduction

It is increasingly believed that local translation in neuronal dendrites is required for long-term synaptic plasticity (Kang and Schuman, 1996; Huber et al., 2000; Martin et al., 2000; Sigrist et al., 2000; Miller et al., 2002; Dubnau et al., 2003). Local translation can be an efficient means for delivering synthesized proteins to the local synapses, which allows selected synapses to control their strength and efficacy independently among thousands of synapses in a neuron (Tiedge et al., 1999; Jiang and Schuman, 2002; Martin and Kosik, 2002). The local translation requires translocation of corresponding mRNAs from the cell bodies to the dendrites, and several mRNAs have been reported to be present in dendrites (Kuhl and Skehel, 1998; Steward and Schuman, 2001). Importantly, some of these mRNAs code key proteins for synaptic plasticity, such as Ca^{2+}/calmodulin-dependent kinase IIα (CaMKIIα) (Burgin et al., 1990), brain-derived neurotrophic factor (BDNF) (Tongiorgi et al., 1997), tyrosine receptor kinase B (TrkB) (Tongiorgi et al., 1997), cAMP response element-binding protein (CREB) (Crino et al., 1998), or NMDA receptor (NMDAR) (Gazzaley et al., 1997). The mRNAs are distributed in the dendrites as granules, which are believed to be identical to "RNA granules." The RNA granules consist of clusters of ribosomes and RNAs and are responsible for mRNA translocation in the dendrites (Knowles et al., 1996; Krichevsky and Kosik, 2001). The RNA granules are reportedly colocalized with translation elongation factor-1α (EF-1α) and staufen (Knowles et al., 1996; Kiebler et al., 1999; Krichevsky and Kosik, 2001), a protein critical for mRNA transport in *Drosophila* development and mammalian neuronal dendrites (Roegiers and Jan, 2000; Tang et al., 2001). However, the constituents of the RNA granules have not been fully identified.

Recent studies have proposed mechanisms of local translation induced by synaptic activation, such as electrical stimulation and BDNF stimulation. These mechanisms include translational initiation by dissociation of eukaryotic initiation factor-4E (eIF-4E)-binding proteins from eIF-4E (Takei et al., 2001; Huang et al., 2002; Jiang and Schuman, 2002; Tang et al., 2002). The dissociation enables eIF-4E, the mRNA 5′ cap-binding protein, to interact directly with eIF-4G, which allows for ribosomal recruitment and translational initiation (Huang et al., 2002; Jiang and Schuman, 2002; Tang et al., 2002). Phosphorylation of eIF-4E by mitogen-activated protein kinase signal-integrating kinase (Mnk), which is associated with eIF-4G, is also induced by BDNF stimulation (Takei et al., 2001). Electron microscopic analysis indicates that the RNA granules are induced to change toward a less compact organization of their ribosomes and release mRNAs during synaptic activation (Krichevsky and Kosik, 2001). The released molecules could then be recruited into polysomes and used for translation.

Here, we show that RNG105 (RNA granule protein 105) is a novel component of the neuronal RNA granules. RNG105 has an ability to bind directly to mRNAs and repress translation. We also

Received Oct. 7, 2004; revised March 17, 2005; accepted March 18, 2005.

This work was supported by the Toray Science Foundation (M.T.), by grants-in-aid from the Ministry of Education, Culture, Sports, Science, and Technology of Japan (MEXT) (N.S., M.T.), by the New Energy and Industrial Technology Development Organization (M.T.), and by the Advanced and Innovational Research Program of MEXT (M.T.). We greatly thank S. Tsukita for support of this study in the initial phase. We thank T. Hirata, Y. Sato, H. Hama, and A. Miyawaki for technical advice, K. Takada, T. Ishikawa, and M. Irie for assistance, J. Ortin for anti-staufen antibody, Y. Mori for GFP-CaMKIIα 3′UTR constructs, and R. Y. Tsien for mRFP1 plasmid.

Correspondence should be addressed to Drs. Nobuyuki Shiina and Makio Tokunaga, Structural Biology Center, National Institute of Genetics, 1111 Yata, Mishima, Shizuoka 411-8540, Japan. E-mail: nshiina@lab.nig.ac.jp and mtoku@lab.nig.ac.jp.

DOI:10.1523/JNEUROSCI.0382-05.2005

 0270-6474/05/254420-15$15.00/0

demonstrate that RNG105 becomes dissociated from the granules by BDNF stimulation, providing insight into the link between RNG105 dynamics and the local translation, which is spatially regulated in the neuronal RNA granules.

Materials and Methods

Reagents and antibodies. The following were used: anti-ribosomal protein S6 (RPS6), anti-eIF-4G, anti-poly(A)-binding protein (PABP) (Santa Cruz Biotechnology, Santa Cruz, CA), anti-microtubule-associated protein 2 (MAP2) (Sigma, St. Louis, MO), anti-postsynaptic density-95 (PSD-95), anti-eIF-4E (BD Biosciences, San Jose, CA), anti-phospho-eIF-4E (Cell Signaling Technology, Beverly, MA), anti-staufen (Marion et al., 1999), anti-EF-1α (Shiina et al., 1994), Alexa 488-labeled anti-rabbit IgG (catalog #A11034; Molecular Probes, Eugene, OR), Alexa 488-labeled streptavidin (catalog #S11223; Molecular Probes), cyanine 3 (Cy3)-labeled anti-mouse IgG (catalog #286343; Jackson ImmunoResearch, West Grove, PA), Cy3-labeled anti-goat IgG (catalog #284733; Jackson ImmunoResearch), Cy3-labeled anti-rabbit IgG (catalog #286753; Jackson ImmunoResearch), rabbit IgG (catalog #011-000-003; Jackson ImmunoResearch), anti-digoxigenin (DIG), Fab fragments (Roche Products, Welwyn Garden City, UK), BDNF, ISOGEN (Wako Chemicals, Osaka, Japan), and RNase inhibitor (catalog #2310; Takara, Shiga, Japan).

To generate specific antibodies against *Xenopus* RNG105 (XRNG105) and RNG105, recombinant proteins were expressed as glutathione *S*-transferase (GST)-tagged fusion proteins in *Escherichia coli* and purified as described previously (Kubo et al., 1999). Antibodies were raised in rabbits and then affinity purified as described previously (Kubo et al., 1999).

cDNA cloning. XRNG105 cDNA was cloned by screening of a λgt11 expression cDNA library of the *Xenopus* oocyte (Clontech, Palo Alto, CA) with one of the monoclonal antibodies (Kubo et al., 1999) and sequenced on both strands as described previously (Shiina and Tsukita, 1999). The sequence data have been submitted to the DNA Data Bank of Japan/European Molecular Biology Laboratory/GenBank databases under accession number AB128031.

Immunoprecipitation and immunoblotting. Rat hippocampal slices were homogenized in 0.25 M sucrose, protease inhibitors (1 mM PMSF, 10 μg/ml leupeptin, pepstatin, aprotinin), 1 mM dithiothreitol (DTT), and 1000 U/ml RNase inhibitor and then centrifuged for 10 min at 10,000 × *g* at 4°C. The supernatant was added at 1:10 vol of 10× PBS followed by 1:20 vol of protein A beads (4 Fast Flow; Amersham Biosciences, Piscataway, NJ), which had been conjugated with anti-RNG105 antibody or control rabbit IgG. After rocking for 2 h at 4°C, the beads were washed three times in PBS containing protease inhibitors and 100 U/ml RNase inhibitor. RNA was extracted from the beads using ISOGEN. Western blotting was performed as described previously (Shiina and Tsukita, 1999).

Cell labeling. Immunoelectron microscopy of cultured *Xenopus* A6 cells with anti-XRNG105 antibody was performed by the silver enhancement method as described previously (Yoshimori et al., 2000). Ultrathin sections (60–90 nm thick) were examined with an electron microscope (JEM 1010; JEOL, Tokyo, Japan).

Cultured cells were immunostained as described previously (Shiina et al., 1992). Rat brains were infused with Tissue-Tek (Sakura Finetek, Tokyo, Japan), frozen in liquid nitrogen, cut into cryosections, and mounted on silan-coated glass coverslips. They were then immunostained as described above. For double immunostaining with anti-RNG105 antibody and antibodies produced in rabbits (anti-staufen, anti-eIF-4G, and anti-phospho-eIF-4E), anti-RNG105 antibody was biotinylated as described previously (Harlow and Lane, 1998). Specimens were stained with the biotinylated anti-RNG105 antibody and Alexa 488-labeled streptavidin after they were stained with the other rabbit antibodies and Cy3-labeled anti-rabbit IgG, refixed with formaldehyde, and blocked with 1 mg/ml rabbit IgG.

For *in situ* hybridization, rat brains were fixed in 4% paraformaldehyde in PBS for 3 h on ice before infusion with Tissue-Tek, and cryosections were mounted as described above. The specimens were refixed in paraformaldehyde for 10 min and dehydrated in 100% ethanol and chloroform for 5 min each and 100% ethanol for 15 min. After rehydration in PBS, specimens were subjected to *in situ* hybridization principally as described previously (Komminoth, 1992; Komminoth et al., 1992), but we omitted the proteinase K treatment and the acetylation steps. DIG-labeled RNA probes were produced from cDNAs using a DIG RNA labeling kit (SP6/T7; Roche Products) and digested to ~100 nucleotides by alkaline treatment. The probes were detected with anti-DIG antibody and Cy3-labeled anti-goat IgG. The specimens were refixed with paraformaldehyde for 10 min, blocked with 1 mg/ml rabbit IgG, and then costained with anti-RNG105 antibody and Alexa 488-labeled anti-rabbit IgG.

For fixed-cell imaging, an FV500 confocal laser-scanning microscope (Olympus Optical, Tokyo, Japan) with a PlanApo 60× oil objective lens was used.

RNA binding of GST-RNG105. To construct the expression vectors for GST-RNG105, GST-ΔC, GST-ΔN1, GST-ΔN2, GST-ΔNC, and GST-CC, RNG105 mRNA from rat brains was amplified by reverse transcription (RT)-PCR and cloned into the *Sal*I and *Not*I sites of pGEX-5X-3 vector (Amersham Biosciences). The primers were 5′-ACGCGTCGACATGAAGCAGATTCTCGGCG-3′ (N-*Sal*I) and 5′-TGCGGCCGCTTAATTCACTTGCTGAGTG-3′ (C-*Not*I) for GST-RNG105, N-*Sal*I and 5′-TGCGGCCGCTTAACTGTTGTAATAAGGCTGACTG-3′ (ΔC-*Not*I) for GST-ΔC, 5′-CGTCGACGATGCCGTATCTAAGTACC-3′ (ΔN-*Sal*I) and C-*Not*I for GST-ΔN1, 5′-CGTCGACGGAGATGATGATGTGAGAAC-3′ and C-*Not*I for GST-ΔN2, ΔN-*Sal*I and ΔC-*Not*I for GST-ΔNC, and 5′-CGTCGACATGAAGCAGATTCTCGGC-3′ and 5′-TGCGGCCGCTTACTGGTCTTGATTGAGCCT-3′ for GST-CC. The recombinant proteins were expressed in *E. coli* (BL21), extracted with PBS containing protease inhibitors, 1 mM DTT, and 0.1% Nonidet P-40, and then bound to glutathione Sepharose beads (4 Fast Flow; Amersham Biosciences). Recombinant protein (10 μg; 3 μg for GST-CC) was bound to 20 μl of beads. The beads were washed five times in the same buffer containing 100 U/ml RNase inhibitor and added at 10 vol of 0.4 mg/ml RNA that had been isolated from rat hippocampus using ISOGEN. After rocking for 20 min at 20°C, the beads were washed three times in the buffer containing 100 U/ml RNase inhibitor. RNA was extracted from the beads using ISOGEN and quantified by measuring absorbance at 260 nm. Poly(dT) (0.1 mg/ml; 55 mer) was preincubated with the isolated RNA for 30 min at 42°C before the addition of the beads. Sense and antisense RNAs of CaMKIIα mRNA were synthesized by *in vitro* transcription from the CaMKIIα coding sequence (CDS) cloned into pGEM-T Easy vector (Promega, Madison, WI) and used at 0.1 mg/ml in the binding assay.

In vitro *translation assay. In vitro* translation was performed in rabbit reticulocyte lysates (L4960; Promega) according to the protocol of the manufacturer. Luciferase mRNA provided with the lysate was used as a template. The CaMKIIα CDS and the green fluorescent protein (GFP)–CaMKIIα 3′ untranslated region (3′UTR) were amplified by PCR from the pGEM-T-CaMKIIα CDS and pC3′full delpCA (Mori et al., 2000) vectors and cloned into the *Xho*I and *Sal*I sites of the pTNT vector (Promega). The primers were 5′-CCGCTCGAGATGGCTACCATCACCTGCACCG-3′ and 5′-ACGCGTCGACATGGGGCAGGACGGAGGGCGCCCC-3′ for the CaMKIIα CDS and 5′-CCGCTCGAGATGGTGAGCAAGGGCGAGGA-3′ and 5′-ACGCGTCGACAAATTTGTAGCTATTTATTCCACTGA-3′ for the GFP-CaMKIIα 3′UTR. CaMKIIα CDS and GFP-CaMKIIα 3′UTR mRNAs were synthesized by *in vitro* transcription from the vectors and used as templates for the *in vitro* translation assay. Incorporation of biotinylated lysine tRNA into luciferase proteins, CaMKIIα proteins, and GFP was detected after SDS-PAGE.

Sucrose density gradient centrifugation and semiquantitative RT-PCR. Rat hippocampal slices were incubated in MEM (M4655; Sigma) in a CO_2 incubator for 50 min with or without BDNF (50 ng/ml). The slices, cultured A6 cells, or rabbit reticulocyte lysates were fractionated by centrifugation through a linear 15–45% sucrose density gradient as described previously (Krichevsky and Kosik, 2001), except that the gradients were prepared using a gradient gel-making device (ATTO, Tokyo, Japan). The samples were fractionated in 25 fractions. RNG105, staufen, and EF-1α were analyzed by Western blotting, and the bands were quantified using NIH Image software. mRNAs were analyzed semiquantitatively by RT-PCR as described previously (Krichevsky and Kosik, 2001).

After agarose gel electrophoresis, the bands were quantified using NIH Image software. Ribosomes were analyzed semiquantitatively by RT-PCR of 18S rRNA. RNA for RT-PCR was extracted using ISOGEN.

Metabolic labeling. Cells (10^7) were labeled for 10 min with 30 μCi/ml [^{35}S]methionine in A6 medium (Shiina and Tsukita, 1999). After washing two times in ice-cold PBS, the cells were lysed in 0.5 ml buffer containing 50 mM Tris-HCl, pH 8.0, 150 mM NaCl, 1% Nonidet P-40, and protease inhibitors. After centrifugation for 10 min at 10,000 × *g* at 4°C, the supernatant was added at an equal volume of 20% TCA (w/v), stored on ice for 15 min, and then centrifuged for 15 min at 10,000 × *g* at 4°C. The precipitants were washed with ice-cold ethanol three times, dried briefly, and dissolved in 20 mM Tris-HCl, pH 8.0, containing 0.5% SDS. They were dissolved in Aquasol 2 (PerkinElmer, Wellesley, MA) and counted using a Liquid Scintillation Analyzer (PerkinElmer).

Plasmid constructs for GFP fusion proteins. To construct the expression vectors for XRNG105-GFP, ΔC-GFP, and ΔN1-GFP, XRNG105 cDNA was amplified by PCR and cloned into the *Hin*dIII and *Kpn*I sites of pEGFP-N1 vector (Clontech). The primers were 5′-CCCAAGCTT-ATGAAACAGATCTTGGGGATC-3′ (N-*Hin*dIII) and 5′-GGGGTAC-CCCGCCTCCATTGACTTGCTGGGGGTTCATC-3′ (C-*Kpn*I) for XRNG105-GFP, N-*Hin*dIII and 5′-GGGGTACCCCTCCTCCAACTGT-TTGTAGCTGCTCTGG-3′ for ΔC-GFP, and 5′-CCCAAGCTTGAT-GCGGTGACAAAACATC-3′ and C-*Kpn*I for ΔN1-GFP. *Xenopus*-cultured A6 cells were transfected with the vectors, and stable transfectants were selected as described previously (Shiina and Tsukita, 1999).

To construct expression vectors for RNG105-GFP and ribosomal L11-GFP, RNG105 and L11 mRNAs from rat brains were amplified by RT-PCR with primers 5′-CGAGCTCATGAAGCAGATTCTCGGCG-3′ and 5′-ACGCGTCGACCCTCCACCACCTCCATTCACTTGCTGAGTGTTC-3′ and with primers 5′-GAAGATCTCATGGCGCAAGATCAGGGT-GAA-3′ and 5′-GCGTCGACTGTTTGCCAGGAAGGATGATGCC-3′, respectively. The products were cloned into the *Sac*I/*Sal*I sites and the *Bgl*II/*Sal*I sites of pEGFP-N1 vector (Clontech), respectively. To construct the expression vector for RNG105-monomeric red fluorescent protein (mRFP1), mRFP1 was amplified by PCR with primers 5′-CCACCGGT-CGCCACCATGGCCTCCTCCGAGGAC-3′ and 5′-ATAAGAATGCG-GCCGCTAGGCGCCGGTGGAGTGGCG-3′ and cloned into the *Age*I and *Not*I sites of the pEGFP-N1-RNG105 vector.

Imaging of living neurons. Hippocampal neurons from embryonic day 18 to embryonic day 20 rats were grown on glass-bottom dishes (Matsunami, Osaka, Japan) and transfected with the vectors by the conventional calcium-phosphate precipitation method. Transection of dendrites was performed as described previously (Aakalu et al., 2001), except that surgical blades (number 11; Feather, Osaka, Japan) were used. Time-lapse images of the cells were taken with an inverted fluorescence microscope (IX71; Olympus Optical) with a PlanApo 60× oil objective lens and a cooled CCD camera (ORCA-ER; Hamamatsu, Shizuoka, Japan).

The fluorescence intensity for each dendrite along its length was measured using NIH Image software. The full width at half-maximum (FWHM) was measured for each RNA granule at $t = -10$ (10 min before BDNF treatment), and the mean pixel intensity within the FWHM was calculated. The FWHM at $t = -10$ was applied to the same granule at every time point. The mean pixel intensity of background (distal and proximal outsides of the FWHM region; 10 μm each) was also calculated and subtracted from the mean pixel intensity within the FWHM region. In Figure 6*C*, The FWHM of RNG105-mRFP1 at $t = -10$ was applied not only to RNG105-mRFP1 but also to L11-GFP in the same granule. To analyze the GFP fluorescence intensity near the RNG105-localizing RNA granules in Figure 7, the mean fluorescence intensity [F_{granule} (F_{g})] of the region containing the RNG105 granule (1.5 μm length) and the mean fluorescence intensity [F_{baseline} (F_{b})] of background (distal and proximal outsides of the RNG105 granule region; 10 μm length each) were calculated. In Figure 7, *E* and *F*, the change in GFP fluorescence intensity was calculated as the following: $[(F_{\mathrm{g}} - F_{\mathrm{b}})_t - (F_{\mathrm{g}} - F_{\mathrm{b}})_{t=-10}]/(F_{\mathrm{g}} - F_{\mathrm{b}})_{t=-10}$, where t is the time after BDNF treatment (in minutes). The images used for the quantitative analyses were not enhanced but were original ones and were without pixel saturation.

Results

RNG105 is a novel protein with an RNA-binding motif

Using one of the monoclonal antibodies raised against *Xenopus* proteins that are associated with centrosomes in a microtubule-dependent manner (Kubo et al., 1999), we identified a protein with an apparent molecular mass of 105 kDa on SDS-PAGE from cultured *Xenopus* A6 cells. Internal peptide sequencing of the purified 105 kDa protein and cDNA isolation revealed that the protein encodes a 680 aa protein (Fig. 1*A*,*B*). We called this protein *Xenopus* RNG105. A database search indicated that XRNG105 may be identical to MP105, a mitotic phosphoprotein of *Xenopus*, for which a partial cDNA sequence has been reported (Stukenberg et al., 1997). Furthermore, XRNG105 has been revealed to be significantly similar to a human protein encoded by a cDNA (GenBank accession number NM_005898; 74.2% identity at the amino acid sequence level). This human RNG105 sequence was originally reported as glycosylphosphatidylinositol (GPI)-anchored membrane protein p137GPI (Ellis and Luzio, 1995) but was replaced recently by the non-GPI-anchored version. The XRNG105 sequence contains no potential sequences for GPI anchor either.

Structural analysis of the XRNG105 sequence predicts an α-helical coiled coil at the N terminus (Fig. 1*A*,*B*). Motifs for both nuclear localization signal (NLS) and nuclear export signal are found, suggesting that XRNG105 can be shuttled between the cytoplasm and the nucleus. A glutamic acid-rich region may be required for the electrostatic interaction of XRNG105 with some molecules. Importantly, XRNG105 contains an RGG box, an RNA-binding motif conserved among a variety of RNA-binding proteins (Burd and Dreyfuss, 1994) (Fig. 1*A*,*B*). In addition, XRNG105 contains a glutamine (Q)-rich region and arginine and glycine (RG)-rich regions, which have been reported in some of the known RNA-binding proteins (Salvetti et al., 1998; Forch et al., 2002). All of these features of XRNG105 are well conserved in vertebrates (data not shown). These findings suggest that XRNG105, and RNG105 in other vertebrates, are RNA-binding proteins.

To examine the subcellular localization and behavior of XRNG105, we immunostained A6 cells with anti-XRNG105 antibody. XRNG105 was visualized as small dots in the cytoplasm (Fig. 1*C*). We further introduced XRNG105 as GFP fusion protein into A6 cells. Expression of XRNG105-GFP (~10-fold of endogenous XRNG105) induced the formation of cytoplasmic granules in which XRNG105 was enriched (Fig. 1*D*). The size of the granules was 0.9 ± 0.5 μm in diameter, which was ~4.5 times larger than control endogenous RNG105 granules (0.2 ± 0.05 μm). Immunoelectron microscopy of A6 cells expressing XRNG105-GFP revealed that spots of XRNG105 immunogold were seen in ribosome-rich areas (Fig. 1*E*). The ribosomes appeared to be distributed homogeneously in the area and not to be clustered closely around the immunogold. We immunostained A6 cells expressing XRNG105-GFP with anti-RPS6 antibody and confirmed that ribosomes were concentrated in the granules (Fig. 1*F*). Furthermore, *in situ* hybridization revealed that mRNAs were also concentrated in the granules (Fig. 1*G* and supplemental Fig. 1, available at www.jneurosci.org as supplemental material). In contrast to XRNG105-GFP, neither XRNG105ΔC-GFP, which lacks the C-terminal RGG box and RG-rich region, nor XRNG105ΔN-GFP, which lacks the N-terminal coiled-coil region, induced the granule formation (Fig. 1*F*,*G*). These results indicate that XRNG105 induces the formation of cytoplasmic granules, which contain ribosomes and mRNAs, and its

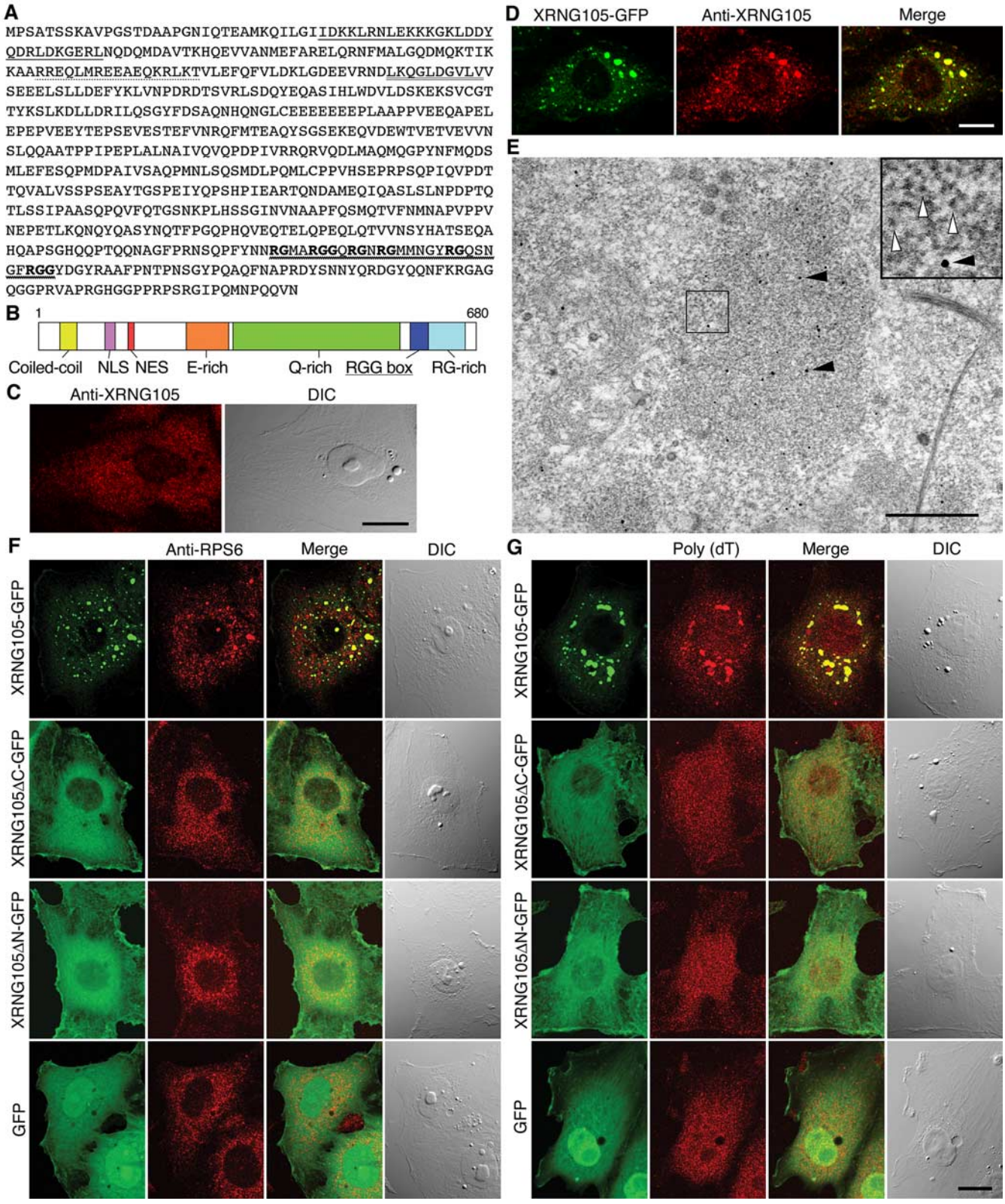

Figure 1. RNG105 is a novel protein with an RNA-binding motif and promotes the organization of cytoplasmic granules containing ribosomes and mRNAs. ***A***, Predicted amino acid sequence of XRNG105. Solid line, Coiled-coil domain; dotted line, NLS; double line, nuclear export signal (NES); wavy line and bold letters, RGG box, an RNA-binding motif. ***B***, Schematic diagram of XRNG105. E-rich, Glutamic acid-rich region; Q-rich, glutamine-rich region; RG-rich, arginine- and glycine-rich region. Other regions are described in ***A***. ***C***, Immunostaining of A6 cells with anti-XRNG105 antibody. Right, Differential interference contrast (DIC) image. Scale bar, 10 μm. ***D***, A6 cells expressing XRNG105-GFP were stained with anti-XRNG105 antibody. Scale bar, 10 μm. Merge, Merged images. ***E***, Immunoelectron microscopy of A6 cells expressing XRNG105-GFP stained with anti-XRNG105 antibody. Spots of immunogold (black arrowheads) are seen in a ribosome-rich area ($\sim$1 μm in diameter) in the cytoplasm. White arrowheads denote ribosomes (inset). Scale bar, 500 nm. ***F***, ***G***, A6 cells expressing XRNG105-GFP, XRNG105ΔC-GFP, XRNG105ΔN-GFP, and GFP were stained with anti-RPS6 antibody (***F***) or stained by *in situ* hybridization with poly(dT) for mRNA detection (***G***). The right panels are DIC images. Scale bar, 10 μm.

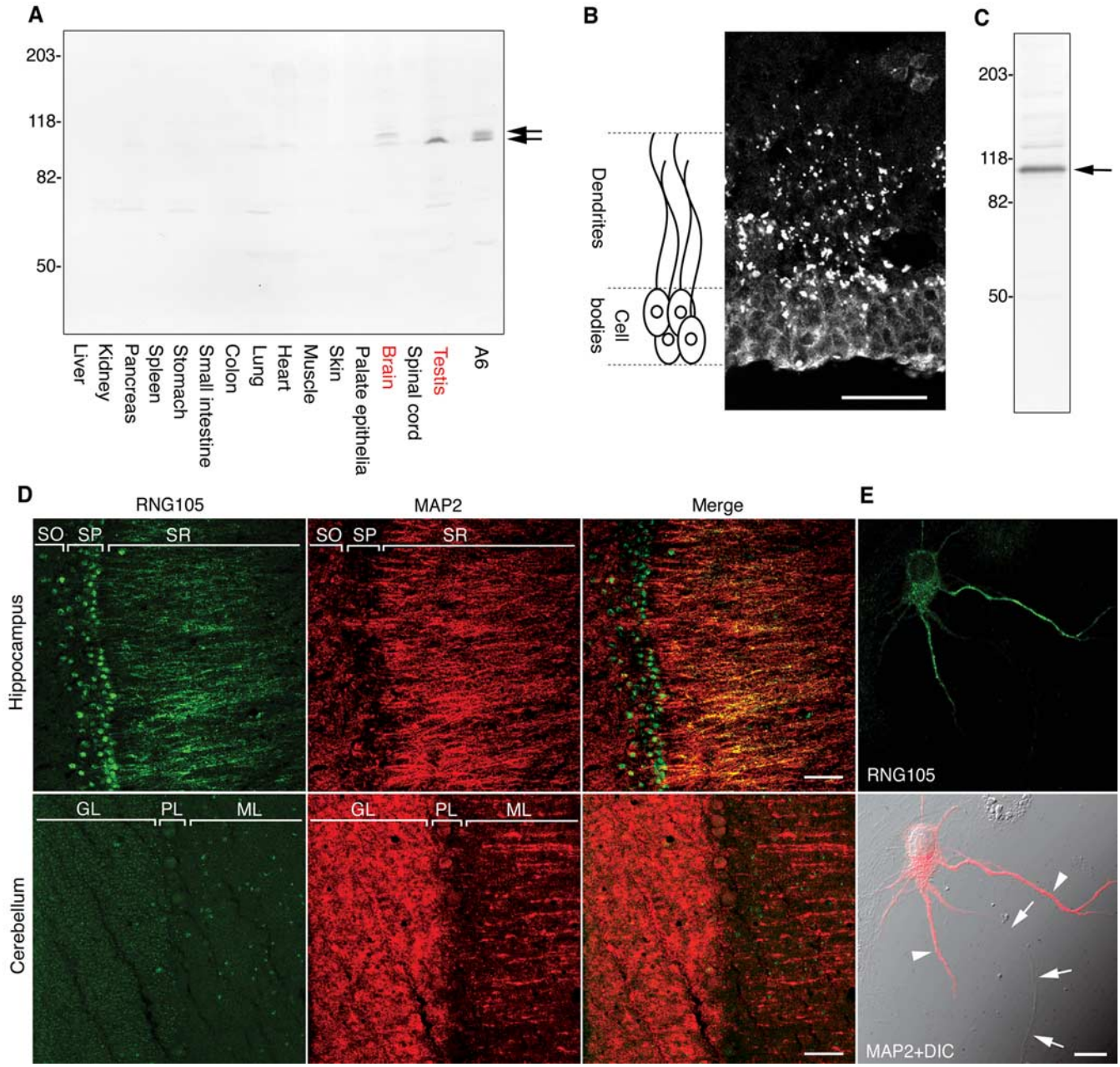

Figure 2. RNG105 is highly expressed in dendrites of hippocampal neurons. ***A***, Western blotting of extracts (30 μg each) from *Xenopus* tissues and A6 cells with anti-XRNG105 antibody. Arrows denote XRNG105. In brain and A6 cells, XRNG105 was detected as doublets, although the reasons for this are not known. ***B***, Immunostaining of slices from the lateral pallium of *Xenopus* forebrain with anti-XRNG105 antibody. A schematic drawing is shown on the left. Scale bar, 50 μm. ***C***, Rat brain extracts were immunoblotted with an antibody directed against mammalian RNG105. Arrow, RNG105. ***D***, Slices from rat hippocampus (top) and cerebellum (bottom) were immunostained with anti-RNG105 antibody (green) and costained with anti-MAP2 antibody, which locates dendrites (red). RNG105 was concentrated in the dendritic region of the stratum radiatum (SR) and in the nuclei of pyramidal neurons [stratum pyramidale (SP)] in the hippocampus. In contrast, RNG105 was not detectable in the dendrites of Purkinje cells in the molecular layer (ML) of the cerebellum. Merge, Merged images; SO, stratum oriens; GL, granule cell layer; PL, Purkinje cell layer. Scale bars, 50 μm. ***E***, Rat cultured hippocampal neurons were immunostained with anti-RNG105 antibody (top) and costained with anti-MAP2 antibody (bottom). Bottom, Composite with a differential interference contrast (DIC) image. Arrowheads indicate dendrites; arrows indicate an axon. Scale bar, 10 μm.

C-terminal RGG box/RG-rich region and N-terminal coiled-coil region are required for the granule formation.

RNG105 is localized in dendrites of hippocampal neurons

The characteristics of the XRNG105-induced granules (i.e., concentration of ribosomes and mRNAs) were most similar to those of the "sponge body" for mRNA transport in *Drosophila* oocytes and RNA granules for mRNA transport in mammalian neurons (Knowles et al., 1996; Wilsch-Brauninger et al., 1997). We then examined tissue specificity of XRNG105 by Western blotting with an anti-XRNG105 polyclonal antibody. XRNG105 was highly expressed in testis and brain (Fig. 2*A*). XRNG105 was highly expressed in the renal cell line A6, although not in kidney (Fig. 2*A*). Similarly, RNG105 from other vertebrates was highly expressed in all of the cultured cell lines we tested, e.g., HeLa, Madin–Darby canine kidney, Chinese hamster ovary, and DT40 cells (data not shown). The expression in cultured cell lines may be attributable to deregulated gene expression in the cultured cells. To examine the localization of XRNG105 in testis and brain, *Xenopus* tissue slices were immunostained with anti-XRNG105

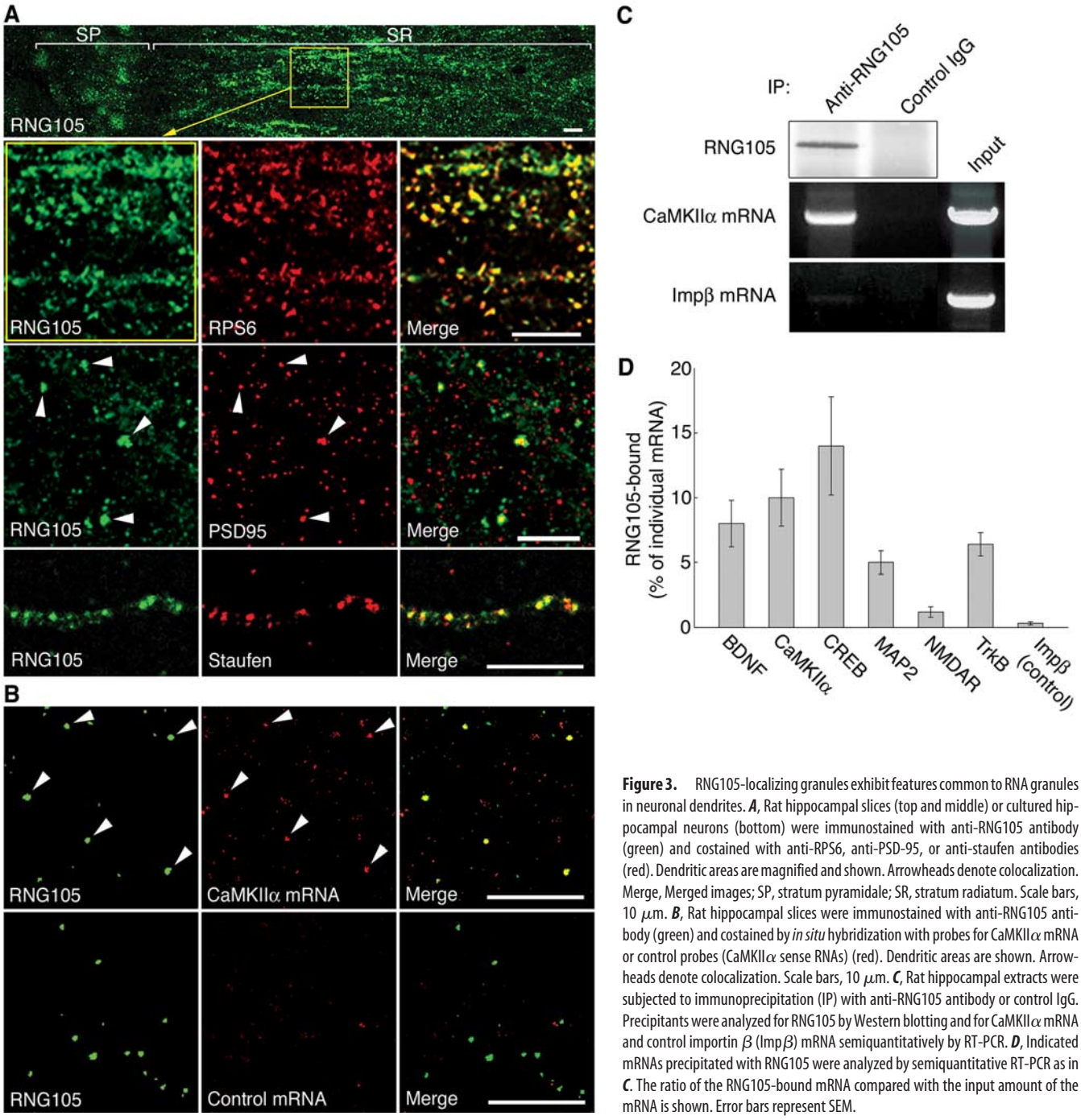

Figure 3. RNG105-localizing granules exhibit features common to RNA granules in neuronal dendrites. ***A***, Rat hippocampal slices (top and middle) or cultured hippocampal neurons (bottom) were immunostained with anti-RNG105 antibody (green) and costained with anti-RPS6, anti-PSD-95, or anti-staufen antibodies (red). Dendritic areas are magnified and shown. Arrowheads denote colocalization. Merge, Merged images; SP, stratum pyramidale; SR, stratum radiatum. Scale bars, 10 μm. ***B***, Rat hippocampal slices were immunostained with anti-RNG105 antibody (green) and costained by *in situ* hybridization with probes for CaMKIIα mRNA or control probes (CaMKIIα sense RNAs) (red). Dendritic areas are shown. Arrowheads denote colocalization. Scale bars, 10 μm. ***C***, Rat hippocampal extracts were subjected to immunoprecipitation (IP) with anti-RNG105 antibody or control IgG. Precipitants were analyzed for RNG105 by Western blotting and for CaMKIIα mRNA and control importin β (Impβ) mRNA semiquantitatively by RT-PCR. ***D***, Indicated mRNAs precipitated with RNG105 were analyzed by semiquantitative RT-PCR as in ***C***. The ratio of the RNG105-bound mRNA compared with the input amount of the mRNA is shown. Error bars represent SEM.

antibody. In testis, XRNG105 was specifically expressed in spermatocytes and spermatids but not in matured sperm (data not shown). In brain, XRNG105 was highly expressed in neurons in the lateral pallium, which is the evolutionary antecedent to the mammalian hippocampus (Fig. 2*B*). In the neurons, XRNG105 was concentrated as granular structures in the cell bodies and the dendritic area (Fig. 2*B*).

We also examined the localization of mammalian RNG105 in rat brain using a polyclonal antibody raised against mammalian RNG105 (Fig. 2*C*). Immunostaining of rat brain slices revealed that RNG105 was concentrated in dendrites of hippocampal neurons (Fig. 2*D*). Higher magnification of the dendritic area showed that RNG105 was localized in granular structures (Fig. 3*A*), as in the case of *Xenopus* brains. The localization of RNG105 in dendrites, but not in axons, was confirmed in cultured hippocampal neurons (Fig. 2*E*). In addition to hippocampal neurons, RNG105 was also concentrated in dendrites of pyramidal neurons in the cerebral neocortex (data not shown). In contrast, RNG105 signal was not detectable in dendrites of Purkinje cells in the cerebellum (Fig. 2*D*). These distinct localizations of RNG105 suggest specific functions of RNG105 in the dendrites of hippocampal and neocortical pyramidal neurons.

Localization of RNG105 in neuronal RNA granules

The localization of RNG105 as granular structures in the neuronal dendrites led us to the idea that the RNG105-localizing granules may be identical to the neuronal RNA granules. We then examined the localization of RNG105 and molecular markers for

the RNA granules in rat hippocampal slices. First, RNG105 was shown to be colocalized with ribosomes in the granular structures (Fig. 3*A*). Quantitative analysis revealed that ~88% of the RNG105-localizing granules were associated with ribosomes. Second, some RNG105-localizing granules (~9%) were accumulated near the postsynaptic sites stained with anti-PSD-95 antibody (Fig. 3*A*), which may be consistent with the previous report that some proportion of polyribosomes is localized near postsynapses (Steward and Levy, 1982). Third, most of the RNG105-localizing granules (~71%) were colocalized with staufen (Fig. 3*A*), a well studied component of the RNA granules (Kiebler et al., 1999; Krichevsky and Kosik, 2001; Tang et al., 2001). These results indicated that the RNG105-localizing granule is identical to the RNA granule in the neuronal dendrites.

Furthermore, we examined the association of the RNG105-localizing granules with CaMKIIα and other mRNAs known to be transported in dendrites. Double staining of rat hippocampal slices showed that ~43% of the RNG105-localizing granules were colocalized with CaMKIIα mRNA (Fig. 3*B*). In addition, immunoprecipitation of RNG105 from rat hippocampal extracts revealed that the precipitants contained a significant amount of CaMKIIα mRNA (Fig. 3*C*,*D*). These results show that RNG105-localizing granules are associated with CaMKIIα mRNA. Using the same methods, BDNF, CREB, MAP2, and TrkB mRNAs were also shown to be associated with the RNG105-localizing granules (Fig. 3*D*). In contrast, NMDAR mRNA was not significantly associated with the granules (Fig. 3*D*), which may be consistent with a previous report that the distribution of NMDAR mRNA in the sucrose density gradient centrifugation was different from those of CaMKIIα and TrkB mRNAs (Krichevsky and Kosik, 2001). These results show that RNG105 is associated with specific dendritic mRNAs in the RNA granules and support the notion that the RNG105-localizing granule is identical to the RNA granule in the neuronal dendrites.

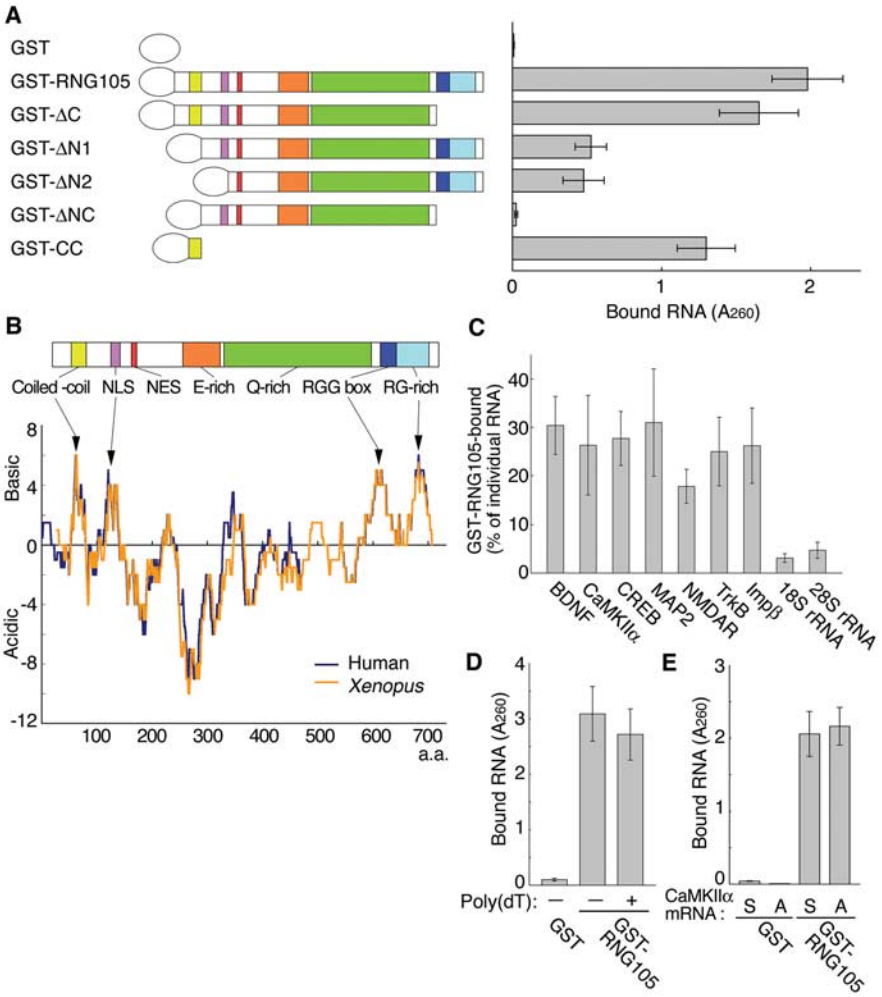

Figure 4. RNG105 binds directly to mRNAs *in vitro*. ***A***, Recombinant GST-RNG105 deletion mutants were incubated with RNAs isolated from rat hippocampus. RNAs bound to the recombinant proteins were extracted and quantified. ΔC, Deletion of C terminus (from RGG box to C-end); ΔN1, deletion of N terminus (from N-end to coiled-coil region); ΔN2, deletion of N terminus (from N-end to NLS); ΔNC, deletion of N and C termini (from N-end to coiled-coil region and from RGG box to C-end); CC, coiled-coil region. ***B***, Acidity–basicity analysis of human and *Xenopus* RNG105. Scores of +1, +0.5, and −1 were given to Lys and Arg, His, and Asp and Glu, respectively. The sum of the scores of 21 aa (residues X − 10 to X + 10) is plotted against a residue number X. Arrows denote clusters of basic residues. NES, Nuclear export signal. ***C***, Indicated RNAs bound to GST-RNG105 in ***A*** were analyzed by semiquantitative RT-PCR. The ratio of the GST-RNG105-bound RNA compared with the input amount of the RNA is shown. Impβ, Importin β. ***D***, Recombinant proteins were incubated with the hippocampal RNAs in the presence or absence of poly(dT), and RNAs bound to the recombinant proteins were quantified. ***E***, Recombinant proteins were incubated with sense (S) or antisense (A) CaMKIIα mRNA, which had been transcribed *in vitro*. Bound RNA was quantified. Error bars represent SEM.

RNG105 binds directly to mRNAs

To examine whether RNG105 has an ability to bind directly to RNA, we constructed recombinant GST-RNG105 and subjected it to an *in vitro* RNA-binding assay. GST-RNG105 was revealed to bind directly to RNA, which had been isolated from rat hippocampus (Fig. 4*A*). The GST-RNG105-bound RNA was also analyzed by semiquantitative RT-PCR. As shown in Figure 4*C*, GST-RNG105 bound to all of the mRNAs tested in this study. It should be noted that GST-RNG105 bound to importin β and NMDAR mRNAs, although these mRNAs were not significantly associated with the RNG105-localizing RNA granules (Fig. 3*D*). The reason for the differences is discussed below. In contrast to the finding that GST-RNG105 binds to mRNAs, it did not bind significantly to 18S or 28S ribosomal RNAs (Fig. 4*C*). Thus, these results indicate that RNG105 has an ability to bind preferentially to mRNAs. Subsequently, we tested whether RNG105 binds to mRNAs via their poly(A) tails. Addition of poly(dT) to mask the poly(A) tails in the *in vitro* binding assay showed that the binding of GST-RNG105 to rat brain RNAs was not significantly altered in the presence or absence of poly(dT), suggesting that poly(A) is not the major binding sequence for RNG105 (Fig. 4*D*). We also tested the possibility that RNG105 binds to mRNAs in a sequence-independent manner. Sense and antisense mRNAs of CaMKIIα CDS were synthesized *in vitro* and used in the *in vitro* binding assay. GST-RNG105 bound to the antisense mRNA as well as the sense mRNA (Fig. 4*E*). These results may indicate that RNG105 binds to mRNAs in a sequence-independent manner or that RNG105 binds to palindromic sequences.

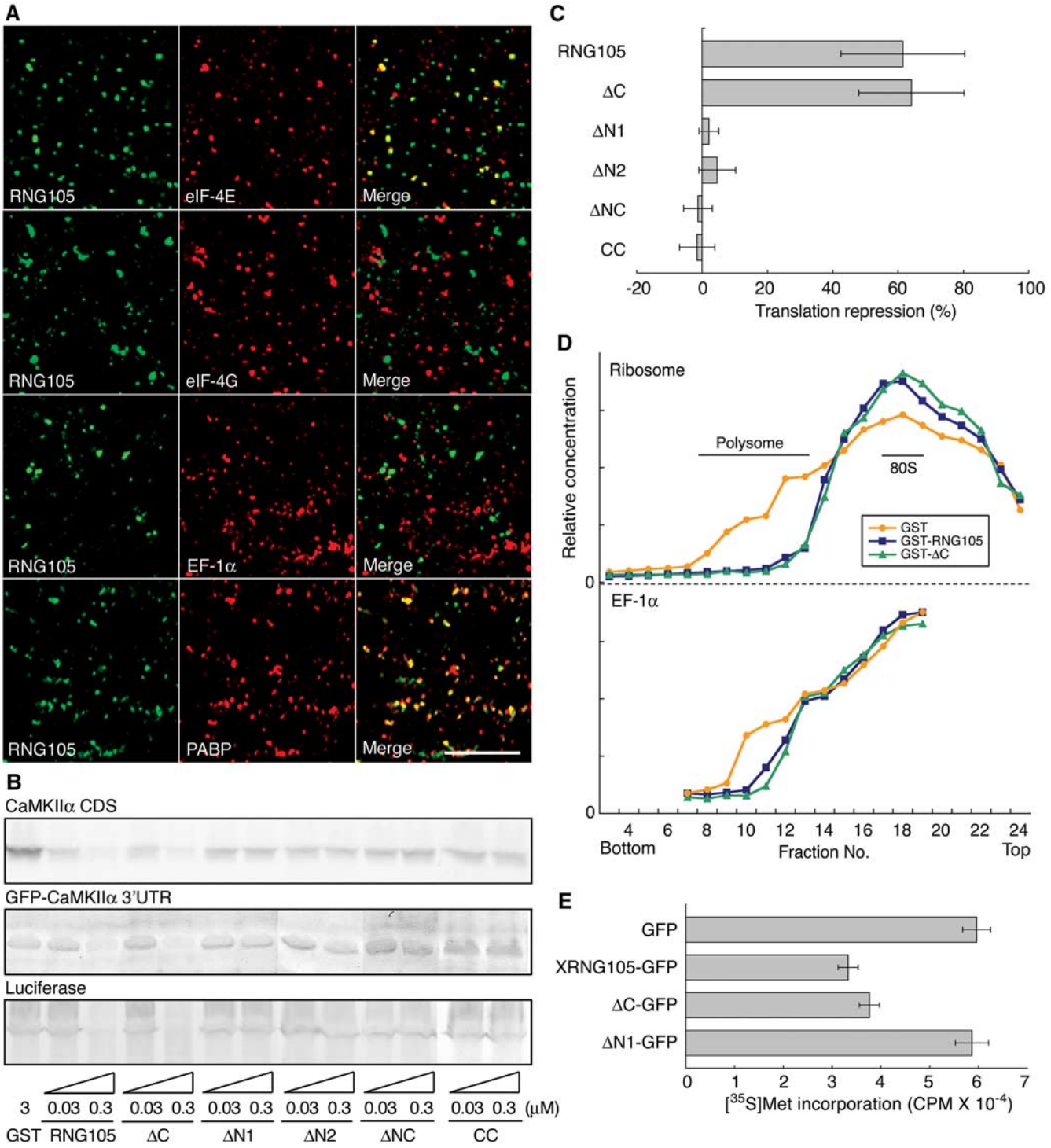

Figure 5. The RNA granule is translationally arrested, and RNG105 negatively regulates translation. ***A***, Rat hippocampal slices were immunostained with anti-RNG105 antibody (green) and costained with anti-eIF-4E, anti-eIF-4G, anti-EF-1α, or anti-PABP antibody (red). Dendritic areas are shown. Merge, Merged image. Scale bar, 10 μm. ***B***, RNG105 inhibits translation *in vitro*. The CaMKIIα CDS, GFP-CaMKIIα 3′ UTR, and luciferase mRNAs were translated in the presence of indicated recombinant proteins in rabbit reticulocyte lysates and detected by SDS-PAGE. CC, Coiled coil. ***C***, The bands in ***B*** were quantified, and translational repression activity of each recombinant protein (0.3 μM) was calculated. Data are means ± SE of translational repression of the three mRNAs by the recombinant proteins. ***D***, The lysates incubated with the recombinant proteins (0.3 μM) in ***B*** were fractionated by sucrose density gradient centrifugation. Elution profiles of ribosomes and EF-1α are shown. ***E***, RNG105 inhibits translation *in vivo*. A6 cells expressing XRNG105-GFP, ΔC-GFP, ΔN1-GFP, or control GFP were labeled with [^{35}S]methionine for 10 min and then proteins were isolated from the cells by TCA precipitation. Incorporation of [^{35}S]methionine ([^{35}S]met) into newly synthesized proteins is shown. CPM, Counts per minute. Error bars represent SEM.

We also constructed GST-RNG105 deletion mutants and tested their binding ability to RNA isolated from rat hippocampus. Deletion of N terminus (GST-ΔN1) markedly reduced, and deletion of C terminus (GST-ΔC) slightly reduced, the RNA-binding ability of RNG105 (Fig. 4*A*). These results indicate that the N terminus containing the coiled-coil region is a major RNA-binding region, and the C terminus containing the RGG box and the RG-rich region is a minor RNA-binding region. Deletion of

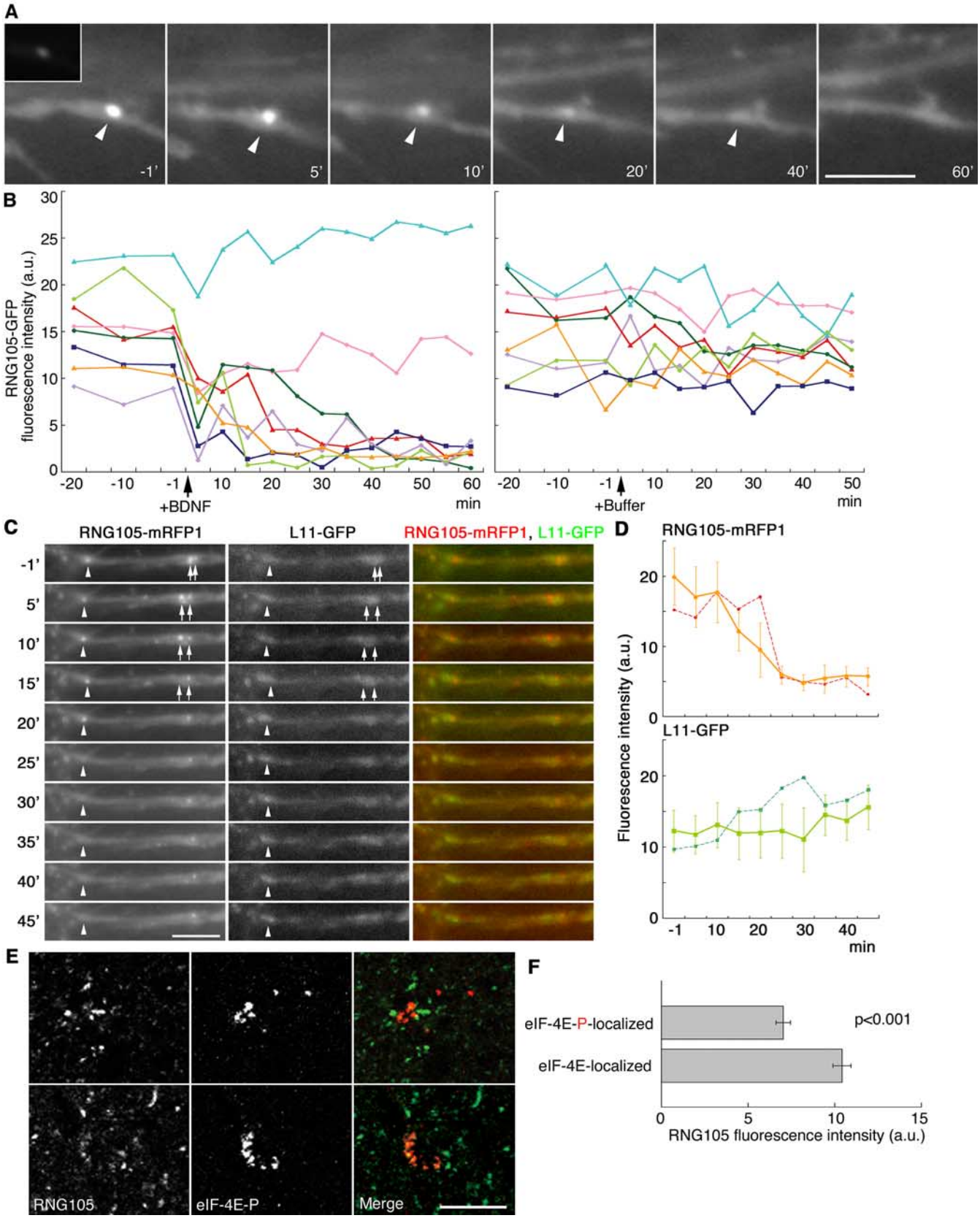

Figure 6. Dissociation of RNG105 from the RNA granules by BDNF stimulation. ***A***, Time-lapse imaging of RNG105-GFP in the dendrites of cultured hippocampal neurons. The time after BDNF treatment is indicated. Arrowheads denote an RNG105-localizing RNA granule, the localization of which was stationary during the imaging period. Enhanced images are shown, and the inset is the original image of the same magnification. Scale bar, 5 μm. ***B***, Left, Profile of RNG105-GFP fluorescence intensity in the granule during the experiment in ***A***. Results obtained from eight granules are shown. RNG105-GFP fluorescence intensity was reduced in the granules, except for those near the cell bodies (pale blue and pink). Right, Control experiments with buffer (PBS) treatment. ***C***, Time-lapse imaging of RNG105-mRFP1 and ribosomal L11-GFP in the dendrites. The time after BDNF treatment is indicated. Arrowheads and arrows denote RNG105-localizing RNA granules, the locations of which were unchanged during the experiment. At the arrowhead and the left arrow, RNG105-mRFP1 signals were significantly reduced after 25 and 15 min, (*Figure legend continues*.)

both of these regions (GST-ΔNC) almost completely lost the binding ability (Fig. 4*A*). The coiled-coil region (GST-CC) was sufficient for the major RNA-binding ability (Fig. 4*A*). Both of these RNA-binding regions (i.e., the coiled-coil region and RGG box/RG-rich region), were revealed to contain clusters of basic amino acid residues (Fig. 4*B*). This structural feature may support the notion that RNG105 binds to RNA via the two regions, mainly via the N-terminal and also via the C-terminal regions.

Translational arrest in RNA granules and repression by RNG105

The RNA granule is reportedly suggested to be in a state of translational arrest because of only trace amounts of eIF-4E and eIF-4G in the RNA granule fractions (Krichevsky and Kosik, 2001). To confirm this, we examined the localization of translation factors in the RNG105-localizing RNA granules in rat hippocampal neurons. Double immunostaining of rat hippocampal slices showed that RNG105-localizing RNA granules were colocalized with eIF-4E and PABP (Fig. 5*A*). Quantitative analysis revealed that ~48 and 83% of the granules were associated with eIF-4E and PABP, respectively. In contrast, most of the RNG105-localizing RNA granules were not colocalized with eIF-4G (Fig. 5*A*). It should be noted that eIF-4G was scattered in the dendrites as granules that were distinct from the RNG105-localizing RNA granules (Fig. 5*A*). We also examined the localization of EF-1α in the granules. EF-1α is reported to be colocalized with some of the RNA granules (Knowles et al., 1996), but we found that EF-1α was localized in granular structures distinct from the RNG105-localizing RNA granules, and only ~1% of the RNG105-localizing RNA granules were associated with EF-1α (Fig. 5*A*). Together, the presence of eIF-4E and PABP supports the finding that the RNG105-localizing RNA granules contain mRNAs, whereas the absence of eIF-4G and EF-1α suggests that the RNG105-localizing RNA granules are in a state of translational arrest.

Subsequently, we tested the effect of RNG105 on translation *in vitro*. Addition of GST-RNG105 in a rabbit reticulocyte lysate system revealed that GST-RNG105 has an ability to repress translation (Fig. 5*B*,*C*). GST-RNG105 (at 0.3 μM) repressed translation of any mRNA we tested (i.e., the CaMKIIα CDS, GFP-CaMKIIα 3′UTR, and luciferase mRNAs), suggesting that the repression may not be sequence specific. GST-ΔC showed translational repression activity similar to that seen for GST-RNG105, whereas GST-ΔN1, GST-ΔN2, or GST-ΔNC showed little activity (Fig. 5*B*,*C*). These results indicate that not the C-terminal but rather the N-terminal region containing the coiled coil is required for the translational repression. However, GST-CC, which contains only the coiled-coil region, did not show the translational repression activity (Fig. 5*B*,*C*), indicating that the coiled-coil region is necessary, but not sufficient, for the translational repression. The rabbit reticulocyte lysate was also subjected to sucrose density gradient centrifugation, and the effect of RNG105 on polysome formation was examined. As shown in Figure 5*D*, addition of GST-RNG105 and GST-ΔC in the reticulocyte lysate reduced ribosomes and EF-1α in the polysome fractions. These results support the finding that RNG105 represses translation in the *in vitro* translation system.

The effect of RNG105 on translation *in vivo* was also examined by expressing XRNG105-GFP in A6 cells. Sucrose density gradient centrifugation of the cells showed that ribosomes and EF-1α in the polysome fractions were reduced by XRNG105-GFP overexpression in the cells (supplemental Fig. 2, available at www.jneurosci.org as supplemental material), which was similar to the finding in the *in vitro* reticulocyte lysate system. In addition, metabolic labeling of the cells with [^{35}S]methionine revealed that protein synthesis in the A6 cells expressing XRNG105-GFP was ~60% of that in control cells expressing GFP (Fig. 5*E*). Expression of ΔC-GFP also reduced the protein synthesis in A6 cells to ~60%, whereas expression of ΔN1-GFP did not reduce the protein synthesis (Fig. 5*E*). These results indicate that RNG105 has an ability to repress translation *in vivo* as well as *in vitro*, and its N terminus is required for the translational repression.

BDNF induces RNG105 release from RNA granules

Local translation in neuronal dendrites is reported to be regulated by synaptic activation. We then examined whether BDNF affects the behavior or distribution of RNG105 in the neuronal dendrites. RNG105-GFP was introduced into cultured hippocampal neurons, and the changes in its behavior and distribution by BDNF stimulation were observed by time-lapse imaging. RNG105-GFP was assembled into the RNA granules in the neurons as in the case in A6 cells. Some granules moved in anterograde and retrograde directions in the dendrites, and the others did not change their locations during the imaging period (data not shown). Interestingly, after BDNF stimulation, RNG105-GFP fluorescence in the RNA granule was markedly reduced (Fig. 6*A*,*B*) compared with control buffer treatment (Fig. 6*B*). These results suggest that the affinity of RNG105 to the RNA granule is reduced by BDNF stimulation. Some of the RNA granules did not show the RNG105-GFP reduction even after BDNF stimulation (Fig. 6*B*, left, pale blue and pink), most likely because the granules were located near the cell bodies in which the cytoplasmic pool of RNG105-GFP was much higher than in distal dendrites. We also introduced ribosomal L11 protein-GFP as a second label for RNA granules in cultured neurons. L11-GFP is reported to be fully functional in yeast (Stage-Zimmermann et al., 2000). In the neurons, L11-GFP fluorescence appeared first in the nucleolus 3–8 h after the transfection and then moved to the cytoplasm and dendrites ~12 h after the transfection, suggesting that L11-GFP was incorporated in 60S ribosomal subunits in the neurons as well as in yeasts. In these neurons, RNG105 was cointroduced as a fusion protein with mRFP1 (Campbell et al., 2002). Distribution of L11-GFP was broader than that of RNG105-mRFP1 in the neuronal dendrites, but L11-GFP was concentrated in and just near the RNG105-localizing RNA granules (Fig. 6*C*). After BDNF stimulation, RNG105-mRFP1 signals were reduced in the RNA granules (Fig. 6*C*,*D*). In contrast, L11-GFP remained unchanged in and near the RNA granules after BDNF stimulation (Fig.

←

(*Figure legend continued*.) respectively. In contrast, L11-GFP signals at the positions were rather constant during the experiment. Scale bar, 5 μm. ***D***, Fluorescence intensities of RNG105-mRFP1 and L11-GFP in the granule denoted by the arrowheads in ***C*** were plotted (dashed lines). Results obtained from eight granules are shown as solid lines (means ± SE). ***E***, ***F***, Rat hippocampal slices were immunostained with anti-RNG105 antibody (***E***, left) and costained with antibody to phosphorylated eIF-4E (eIF-4E-P; ***E***, middle). Although the slices were not treated with BDNF, some areas were stained with anti-eIF-4E-P antibody, which may be because these areas had been activated when the animals were alive. Dendritic areas are shown. RNG105 fluorescence in the granules in which eIF-4E-P was localized was relatively faint compared with that in other RNA granules. ***F***, Fluorescence intensity of RNG105 in the eIF-4E-P-localizing granules was measured and compared with that in the eIF-4E-localizing granules. a.u., Arbitrary units. Scale bar, 10 μm. Error bars represent SEM.

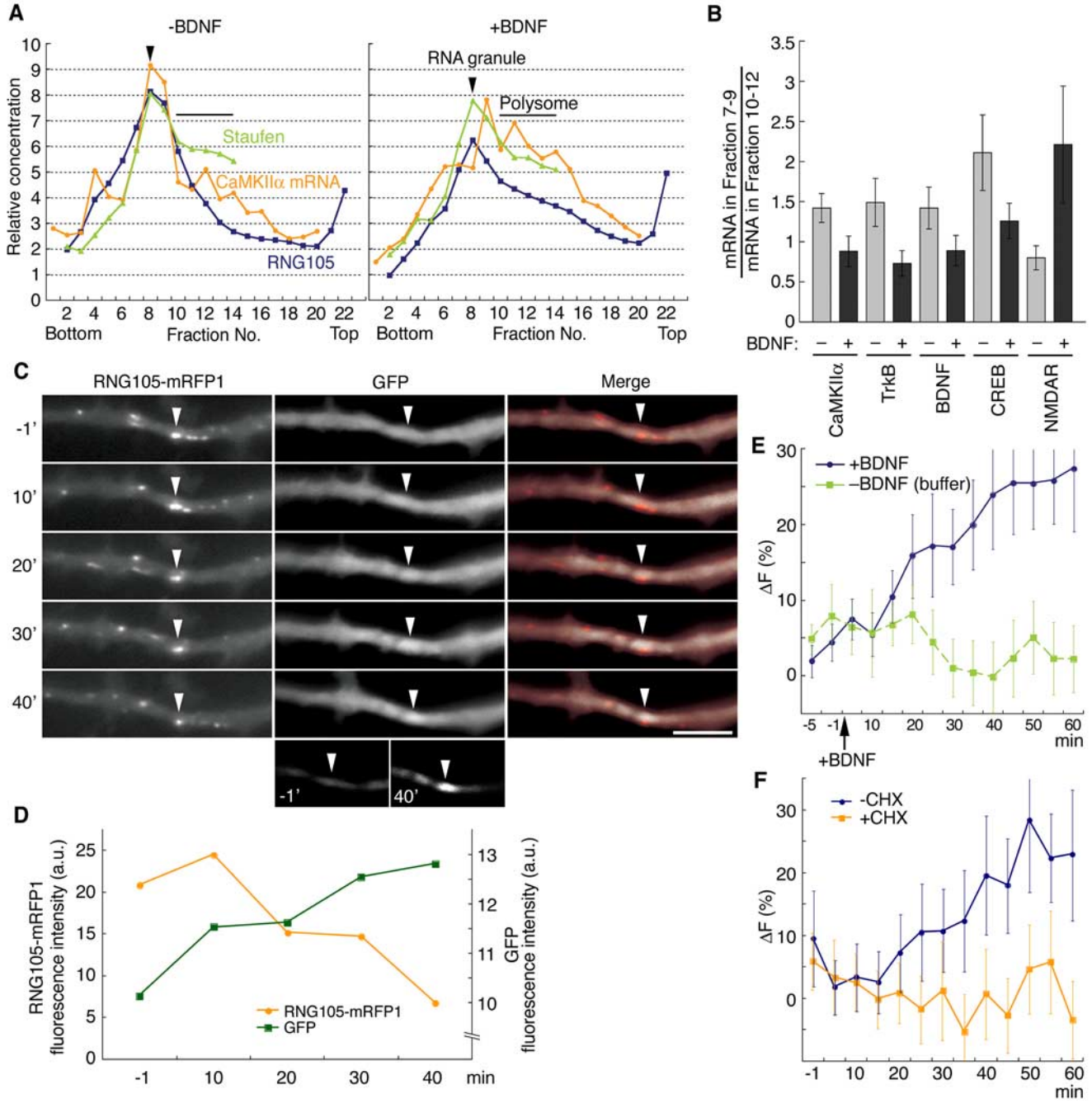

Figure 7. BDNF induces mRNA shift from the RNA granules to polysomes and local translation near the granules. ***A***, Extracts from control or BDNF-stimulated rat hippocampal slices were fractionated by sucrose density gradient centrifugation and then RNG105, staufen, and CaMKIIα mRNA were analyzed semiquantitatively (means from 3 independent experiments). ***B***, The indicated mRNAs were analyzed as in ***A***. The ratios of the mRNA in the RNA granule fractions to that in the lighter fractions (polysomes) are shown. ***C***, Rat cultured hippocampal neurons were transfected with both GFP reporter fused to the CaMKIIα 3′ UTR and RNG105-mRFP1. Time-lapse images of GFP and RNG105-mRFP1 proteins after BDNF stimulation are shown. Arrowheads denote the position of a granule with a stationary localization during the imaging period. RNG105-mRFP1 in the granule was reduced after BDNF stimulation, which coincided with the increase in GFP signal near the granule. To image clearly the increase in GFP signal near the granules, enhanced images of the GFP signal −1 and 40 min after the stimulation are shown at the bottom. Other granules were motile and changed their positions during the experiment. Scale bar, 5 μm. ***D***, Profiles of RNG105-mRFP1 and GFP fluorescence intensity in the granule indicated by arrowheads in ***C***. a.u., Arbitrary units. ***E***, Profile of GFP fluorescence changes during the experiment in ***C***. The changes in GFP fluorescence intensities near the RNG105-localizing RNA granules between the indicated time points and $t = -10$ min are plotted. Data are means ± SE from eight granules of two independent experiments. ***F***, The same experiment as in ***E***, except for the addition of 10 μg/ml cycloheximide (CHX) 10 min before the BDNF stimulation. Error bars represent SEM.

6*C*,*D*). These results indicate that the RNA granules remained in place over the imaging period, but RNG105 was released from the RNA granules after BDNF stimulation.

We also examined the colocalization of RNG105 with phosphorylated eIF-4E, the phosphorylation of which is induced by BDNF (Takei et al., 2001). Because the phosphorylation of eIF-4E is catalyzed by Mnk, which is associated with eIF-4G (Scheper and Proud, 2002), eIF-4E phosphorylation suggests its association with eIF-4G. Immunostaining of hippocampal slices revealed that the RNG105 signals in the granules in which phosphorylated eIF-4E was located were relatively faint compared with those in other RNA granules (Fig. 6*E*). Quantitative analysis

showed that RNG105 in the phosphorylated eIF-4E-localizing granules was significantly reduced (Fig. 6*F*). These results suggest that RNG105 release from the RNA granules is coincident with eIF-4E phosphorylation, which is induced by BDNF and suggests the association of eIF-4E with eIF-4G.

Local translation near RNA granules induced by BDNF

We also examined the effect of BDNF on the affinity of mRNAs as well as RNG105 to the RNA granules by sucrose density gradient centrifugation. As shown in Figure 7*A*, without BDNF stimulation, the peak fraction of CaMKIIα mRNA corresponded significantly to the peak of RNG105 and staufen, indicating again that RNG105 and CaMKIIα mRNA are colocalized in the RNA granules. In contrast, after BDNF stimulation, CaMKIIα mRNA shifted to lighter fractions corresponding to polysomes (Fig. 7*A*). These results were consistent with the previous study indicating that mRNAs in the RNA granules shift to polysomes after synaptic activation (Krichevsky and Kosik, 2001). The amount of RNG105 in the RNA granule fractions was reduced after BDNF stimulation (Fig. 7*A*), which is consistent with the finding that the affinity of RNG105 to the RNA granule is reduced by BDNF stimulation (Fig. 6). In contrast, the amount of staufen in the RNA granule fractions was not reduced after BDNF stimulation (Fig. 7*A*), consistent with the finding that ribosomal L11 remained in and near the RNA granules after BDNF stimulation (Fig. 6*C*,*D*). It should be noted that, after BDNF stimulation, CaMKIIα mRNA peaks did not correspond to any peaks for RNG105 (Fig. 7*A*). Thus, these results suggest that CaMKIIα mRNA is released from RNG105 and shifts to polysomes under the control of BDNF. Using the same method, TrkB, BDNF, and CREB mRNAs were also shown to shift from the RNA granule fractions to the lighter fractions after BDNF stimulation (Fig. 7*B*). In contrast, NMDAR mRNA, which was shown not to be associated significantly with the RNA granules (Fig. 3*D*), did not show such a shift after BDNF stimulation (Fig. 7*B*).

The shift of mRNAs from the RNA granules to polysomes suggested translational induction of the mRNAs. Subsequently, we transfected cultured hippocampal neurons with a GFP reporter gene and examined whether the translation of the GFP reporter is induced by BDNF stimulation. The GFP reporter gene was fused to the full length of CaMKIIα 3′UTR, which is sufficient for its mRNA to be transported into dendrites (Mori et al., 2000). The hippocampal neurons were cotransfected with RNG105-mRFP1 to locate the RNG105-localizing RNA granules. Real-time imaging revealed that the GFP signal intensity was significantly increased near RNG105-mRFP1 in the dendrites after BDNF stimulation (Fig. 7*C*–*E*). The increase in GFP signal was coincident with the decrease in RNG105-mRFP1 in the RNA granules (Fig. 7*C*,*D*). Application of the translational inhibitor cycloheximide blocked the increase in GFP signal near RNG105-mRFP1, indicating that the increased GFP signal was attributable to protein synthesis (Fig. 7*F*).

To determine whether this translation occurs locally, the dendrites were severed from the cell body (supplemental Fig. 3*A*, available at www.jneurosci.org as supplemental material). In these transected dendrites, cytoplasmic GFP background was decreased and GFP signals were detected as fine dots like RNG105 signals (supplemental Fig. 3*B*, available at www.jneurosci.org as supplemental material). The GFP signals were colocalized with RNG105-mRFP1 and increased after BDNF stimulation (supplemental Fig. 3*B*,*C*, available at www.jneurosci.org as supplemental material). The increase in GFP signal was blocked by application of cycloheximide (supplemental Fig. 3*B*,*C*, available at www.jneurosci.org as supplemental material). These results indicate that the translation is induced locally in the dendrites.

The increase in GFP signals near the RNG105-localizing granules was consistent with previous reports that local translation of the GFP reporter was induced by BDNF (Aakalu et al., 2001; Job and Eberwine, 2001). Together, these results suggest that BDNF induces the release of mRNAs from RNG105 and the mRNA shift to polysomes and subsequent translation in the vicinity of the RNA granules.

Discussion

RNG105 is a novel RNA-binding protein in neuronal RNA granules

This study has identified RNG105, a novel protein component of the RNA granules in the dendrites of hippocampal neurons. RNG105 was shown to bind directly to mRNAs in a sequence-independent manner *in vitro* and repress translation *in vitro* and *in vivo*. The N terminus of RNG105 was required for the mRNA binding and translational repression. The N terminus contains a coiled coil with clusters of basic residues, and this region was sufficient for its major RNA-binding ability. Similar structure in aminoacyl-tRNA synthetases is reported (Cahuzac et al., 2000). This structure is an antiparallel coiled coil with a basic patch, presenting a suitable docking surface for nucleic acids. Its binding to RNA is shown to be neither sequence nor structure specific. RNG105 could bind to RNA in a manner similar to that seen for these proteins. Although the coiled-coil region (GST-CC) bound to RNA, the region did not show the translational repression, indicating that the binding of the coiled-coil region to mRNA is not sufficient, and other additional regions are required for the repression. The additional regions may not be the C-terminal RGG box/RG-rich region, a minor RNA-binding region, because the ΔC construct showed translational repression activity as well as the full-length RNG105. The translational repression by RNG105 was also sequence independent. Some translational repressors, e.g., cytoplasmic polyadenylation element-binding protein (CPEB), are reportedly bound to specific sequences in 3′UTR to repress translation (Huang et al., 2002; Jiang and Schuman, 2002), but RNG105 repressed the translation of CaMKIIα mRNA independently on its 3′UTR. Some RNA-binding proteins are also known to bind to mRNAs in a sequence-independent manner and repress translation. For example, mouse MSY1 and *Xenopus* FRGY2 are present in messenger ribonucleoprotein (mRNP) particles and function to mask mRNAs to inhibit translation in germ cells (Wolffe, 1994). Both the N terminus and the C terminus of RNG105 were required for the formation of the granules [i.e., its association with the RNA granules in A6 cells (Fig. 1*F*,*G*) and cultured hippocampal neurons (data not shown)]. Thus, RNG105 is a novel type of RNA-binding protein in the neuronal RNA granules.

Although the binding of RNG105 to mRNAs was sequence independent *in vitro*, RNG105 was shown in hippocampal slices to be associated with specific mRNAs, the translational products of which are key molecules for synaptic plasticity. The different mRNA specificity between *in vitro* and *in vivo* may be explained by the specificity of RNG105 to mRNAs being controlled in the RNA granules or, in contrast, may indicate that other RNA-binding proteins in the RNA granules may determine the mRNA specificity. In the latter case, although RNG105 may not be the determinant for the mRNA specificity in the neuronal RNA granules, the association of RNG105 with the granules via its N and C termini would enable the N terminus to bind to specific mRNAs in the granules recruited by other RNA-binding protein(s). As a

result, RNG105 would bind to and repress translation of specific mRNAs in the RNA granules (supplemental Fig. 4, available at www.jneurosci.org as supplemental material). The deletion mutant of the C terminus, ΔC, cannot assemble into the RNA granules but can inhibit translation *in vitro* and in A6 cells. This finding may be explained by the translational repression activity of RNG105 not requiring its association with the granules. The property of RNG105 to be associated with the granules may be required for meeting specific mRNAs in the granules.

Translation factors in the RNA granules

In this study, eIF-4E and PABP were associated with the RNG105-localizing RNA granules. These translation factors may bind directly to mRNAs in the granules. In contrast, eIF-4G or EF-1α was not associated with the granules, indicating that the RNG105-localizing RNA granule is in a state of translational arrest, which is consistent with a previous report (Krichevsky and Kosik, 2001). However, it is reported that EF-1α is localized in the RNA granules (Knowles et al., 1996). In addition, a recent study demonstrated that BDNF treatment increases eIF-4E association with cytoskeletally bound RNA granules in an actin- and integrin-dependent manner (Smart et al., 2003). These reports suggest that RNA granules are translationally active locations, which is not consistent with our results and the previous report (Krichevsky and Kosik, 2001) that BDNF induces the shift of mRNAs from the RNA granules to polysomes. One possible explanation for these differences is that there could be multiple RNA granule populations with different compositions and roles in synaptic activation. RNG105-localizing RNA granules could be translationally arrested among the various RNA granules.

It is widely accepted that ribosomes are localized in the RNA granules, and we show here that RNG105-localizing RNA granules contain ribosomes. Because the RNG105-localizing RNA granules do not contain eIF-4G and are suggested to be translationally arrested, it is unlikely that the ribosomes are associated with mRNAs through eIF-4G as translationally competent complexes in the granules. Ribosomes may be localized in the RNA granules as untranslating ribosomes and/or ribosomal subunits, and the localization may not depend on eIF-4E/4G or mRNAs, as illustrated by Krichevsky and Kosik (2001).

A model for the regulation of local translation

RNG105 has been suggested to be associated with the RNA granules via its N and C termini and bind to and repress the translation of mRNAs via its N terminus. Consistent with the ability of RNG105 to repress translation, the RNG105-localizing RNA granules were shown to be translationally arrested in the basal conditions. In contrast, after synaptic stimulation by BDNF, RNG105 was released from the RNA granules, which coincided with the mRNA shift to polysomes and translational induction near the granules. Based on these results, we suggest that RNG105 may be involved in BDNF-regulated local translational control (supplemental Fig. 4, available at www.jneurosci.org as supplemental material). In this model, RNG105 is associated with RNA granules via its N and C termini. In the granules, RNG105 directly binds to mRNAs via its N terminus, which would repress translation of the mRNAs localized in the RNA granules. After BDNF stimulation, the affinity of RNG105 to the granules would be reduced, which would lead to the dissociation of RNG105 from the granules. The RNG105 dissociation from the granules is concomitant with increased local translation near the granules. The molecular mechanism whereby the RNG105 dissociation is related to the transformation of RNA granules into translating polysomes and to the increase in local translation is an important question to be answered in future studies.

It is noteworthy that RNG105 can be phosphorylated in mitosis (Stukenberg et al., 1997). In addition, in mitosis, XRNG105-GFP becomes dissociated from the granular structures in A6 cells (our unpublished data). This suggests that RNG105 may be phosphorylated by a kinase(s), activated in mitosis and by synaptic stimulation, which may reduce the ability of RNG105 to bind to RNA granules and mRNAs. It is reported that a GPI-anchored protein, which has been replaced by a non-GPI-anchored version and is identical to RNG105, is associated with receptor for activated protein kinase C (PKC) 1 (RACK1), which is part of mRNP complexes and localized in neuronal dendrites and dendritic spines (Angenstein et al., 2002). This association was not followed up, probably because of the misattribution of the protein as a GPI-anchored protein. Because RACK1 is shown to be associated with ribosomes and provide a link between PKC signaling and ribosomal subunit joining (Ceci et al., 2003), it would be interesting to see whether RNG105 is regulated by RACK1/PKC and involved in ribosome assembly.

In addition to the inhibitory mechanism by RNG105, there are mechanisms that activate translation by phosphorylation of translation factors (Martin et al., 2000; Takei et al., 2001; Jiang and Schuman, 2002). All of these mechanisms should be regulated by synaptic stimulation so that the local translation of the mRNAs in the RNA granules can be increased.

CPEB is reported to be responsible for stimulation-dependent local translation in neuronal dendrites (Huang et al., 2002; Jiang and Schuman, 2002). It controls translation of specific mRNAs with CPE sequences. Among the mRNAs, which are shown in this study to be localized with RNG105 in the RNA granules, only CaMKIIα and MAP2 mRNAs contains the CPE, whereas others do not. Therefore, CPEB may not target these mRNAs, except for CaMKIIα and MAP2. CPEB is reported to be localized mainly at the postsynaptic density using immunofluorescence and cell fractionation methods (Huang et al., 2002). In contrast, in this study, we show that RNG105 is localized in the RNA granules, and only a small proportion of them are associated with the postsynaptic sites. Thus, RNG105 and CPEB are likely to play their roles at different locations in the dendrites. RNG105 would play important roles in local translational control at the postsynaptic sites and, in addition, in translational repression in the RNA granules during transport of mRNAs in the dendrites.

Specific roles of RNG105 in vertebrates and insects

Recent studies have revealed mRNA translocation and local protein synthesis in different organisms and cell types, such as *Drosophila* oocytes, germ cells, neurons, *Xenopus* oocytes, cultured fibroblasts, and mammalian neurons (St Johnston, 1995; Lipshitz and Smibert, 2000; Kloc et al., 2002). Importantly, the mechanisms for the local translation that we proposed in this study are likely to be shared among various organisms and cell types (Kedersha et al., 2000; Lipshitz and Smibert, 2000; Krichevsky and Kosik, 2001). Therefore, the translational regulation in the RNA granules should provide a general model for the regulation of local translation. RNG105 is highly conserved among vertebrates, and its N terminus is conserved in *Drosophila* (GenBank accession number NM_144414) (data not shown). Although the C terminus of the *Drosophila* homolog is not similar to vertebrate RNG105, it contains a Q-rich region and an RGG box (data not shown), suggesting that the homolog has functions similar to vertebrate RNG105. RNG105 homologs were not found in yeast or *Caenorhabditis elegans*. RNG105 was expressed mainly in tes-

tis, oocyte, and brain tissues, in which RNG105 was localized in dendrites of hippocampal and neocortical pyramidal neurons but not in dendrites of Purkinje cells. Thus, the activity of RNG105 is likely to be tissue specific and restricted to vertebrates and insects.

In this study, we showed that RNG105 has an ability to bind to mRNAs and repress translation. RNG105 is associated with the RNA granules in neuronal dendrites, and its affinity to the granules is controlled by BDNF stimulation. In summary, RNG105 is suggested to be implicated in a key role in the local translational regulation in the neuronal RNA granules and to control synaptic plasticity in an activity-dependent manner.

References

Aakalu G, Smith WB, Nguyen N, Jiang C, Schuman EM (2001) Dynamic visualization of local protein synthesis in hippocampal neurons. Neuron 30:489–502.

Angenstein F, Evans AM, Settlage RE, Moran ST, Ling S-C, Klintsova AY, Shabanowitz J, Hunt DF, Greenough WT (2002) A receptor for activated C kinase is part of messenger ribonucleoprotein complexes associated with polyA–mRNAs in neurons. J Neurosci 22:8827–8837.

Burd CG, Dreyfuss G (1994) Conserved structures and diversity of functions of RNA-binding proteins. Science 265:615–621.

Burgin KE, Waxham MN, Rickling S, Westgate SA, Mobley WC, Kelly PT (1990) *In situ* hybridization histochemistry of Ca^{2+}/calmodulin-dependent protein kinase in developing rat brain. J Neurosci 10:1788–1798.

Cahuzac B, Berthonneau E, Birlirakis N, Guittet E, Mirande M (2000) A recurrent RNA-binding domain is appended to eukaryotic aminoacyl-tRNA synthetases. EMBO J 19:445–452.

Campbell RE, Tour O, Palmer AE, Steinbach PA, Baird GS, Zacharias DA, Tsien RY (2002) A monomeric red fluorescent protein. Proc Natl Acad Sci USA 99:7877–7882.

Ceci M, Gaviraghi C, Gorrini C, Sala LA, Offenhauser N, Marchisio PC, Biffo S (2003) Release of eIF6 ($p27^{BBP}$) from the 60S subunit allows 80S ribosome assembly. Nature 426:579–584.

Crino P, Khodakhah K, Becker K, Ginsberg S, Hemby S, Eberwine J (1998) Presence and phosphorylation of transcription factors in developing dendrites. Proc Natl Acad Sci USA 95:2313–2318.

Dubnau J, Chiang A-S, Grady L, Barditch J, Gossweiler S, McNeil J, Smith P, Buldoc F, Scott R, Certa U, Broger C, Tully T (2003) The *staufen/pumilio* pathway is involved in *Drosophila* long-term memory. Curr Biol 13:286–296.

Ellis JA, Luzio JP (1995) Identification and characterization of a novel protein (p137) which transcytoses bidirectionally in Caco-2 cells. J Biol Chem 270:20717–20723.

Forch P, Puig O, Martinez C, Seraphin B, Valcarcel J (2002) The splicing regulator TIA-1 interacts with U1-C to promote U1 snRNP recruitment to 5′ splice sites. EMBO J 21:6882–6892.

Gazzaley AH, Benson DL, Huntley GW, Morrison JH (1997) Differential subcellular regulation of NMDAR1 protein and mRNA in dendrites of dentate gyrus granule cells after perforant path transection. J Neurosci 17:2006–2017.

Harlow E, Lane D (1998) Labeling antibodies with biotin. In: Antibodies, pp 340–341. New York: Cold Spring Harbor Laboratory.

Huang Y-S, Jung M-Y, Sarkissian M, Richter JD (2002) *N*-methyl-D-aspartate receptor signaling results in Aurora kinase-catalyzed CPEB phosphorylation and αCaMKII mRNA polyadenylation at synapses. EMBO J 21:2139–2148.

Huber KM, Kayser MS, Bear MF (2000) Role for rapid dendritic protein synthesis in hippocampal mGluR-dependent long-term depression. Science 288:1254–1256.

Jiang C, Schuman EM (2002) Regulation and function of local protein synthesis in neuronal dendrites. Trends Biochem Sci 27:506–513.

Job C, Eberwine J (2001) Identification of sites for exponential translation in living dendrites. Proc Natl Acad Sci USA 98:13037–13042.

Kang H, Schuman EM (1996) A requirement for local protein synthesis in neurotrophin-induced hippocampal synaptic plasticity. Science 273:1402–1406.

Kedersha N, Cho MR, Li W, Yacono PW, Chen S, Gilks N, Golan DE, Anderson P (2000) Dynamic shuttling of TIA-1 accompanies the recruitment of mRNA to mammalian stress granules. J Cell Biol 151:1257–1268.

Kiebler MA, Hemraj I, Verkade P, Kohrmann M, Fortes P, Marion RM, Ortin J, Dotti CG (1999) The mammalian staufen protein localizes to the somatodendritic domain of cultured hippocampal neurons: implications for its involvement in mRNA transport. J Neurosci 19:288–297.

Kloc M, Zearfoss NR, Etkin LD (2002) Mechanisms of subcellular mRNA localization. Cell 108:533–544.

Knowles RB, Sabry JH, Martone ME, Deerinck TJ, Ellisman MH, Bassell GJ, Kosik KS (1996) Translocation of RNA granules in living neurons. J Neurosci 16:7812–7820.

Komminoth P (1992) Digoxigenin as an alternative probe labeling for *in situ* hybridization. Diagn Mol Pathol 1:142–150.

Komminoth P, Merk FB, Leav I, Wolfe HJ, Roth J (1992) Comparison of ^{35}S- and digoxigenin-labeled RNA and oligonucleotide probes for *in situ* hybridization. Expression of mRNA of the seminal vesicle secretion protein II and androgen receptor genes in the rat prostate. Histochemistry 98:217–228.

Krichevsky AM, Kosik KS (2001) Neuronal RNA granules: a link between RNA localization and stimulation-dependent translation. Neuron 32:683–696.

Kubo A, Sasaki H, Yuba-Kubo A, Tsukita S, Shiina N (1999) Centriolar satellites: molecular characterization, ATP-dependent movement toward centrioles and possible involvement in ciliogenesis. J Cell Biol 147:969–979.

Kuhl D, Skehel P (1998) Dendritic localization of mRNAs. Curr Opin Neurobiol 8:600–606.

Lipshitz HD, Smibert CA (2000) Mechanisms of RNA localization and translational regulation. Curr Opin Genet Dev 10:476–488.

Marion RM, Fortes P, Beloso A, Dotti C, Ortin J (1999) A human sequence homologue of staufen is an RNA-binding protein that is associated with polysomes and localizes to the rough endoplasmic reticulum. Mol Cell Biol 19:2212–2219.

Martin KC, Kosik KS (2002) Synaptic tagging—who's it? Nat Rev Neurosci 3:813–820.

Martin KC, Barad M, Kandel ER (2000) Local protein synthesis and its role in synapse-specific plasticity. Curr Opin Neurobiol 10:587–592.

Miller S, Yasuda M, Coats JK, Jones Y, Martone ME, Mayford M (2002) Disruption of dendritic translation of CaMKIIα impairs stabilization of synaptic plasticity and memory consolidation. Neuron 36:507–519.

Mori Y, Imaizumi K, Katayama T, Yoneda T, Tohyama M (2000) Two cis-acting elements in the 3′ untranslated region of α-CaMKII regulate its dendritic targeting. Nat Neurosci 3:1079–1084.

Roegiers F, Jan YN (2000) Staufen: a common component of mRNA transport in oocytes and neurons? Trends Cell Biol 10:220–224.

Salvetti A, Batistoni R, Deri P, Rossi L, Sommerville J (1998) Expression of DjY1, a protein containing a cold shock domain and RG repeat motifs, is targeted to sites of regeneration in planarians. Dev Biol 201:217–229.

Scheper GC, Proud CG (2002) Does phosphorylation of the cap-binding protein eIF4E play a role in translation initiation? Eur J Biochem 269:5350–5359.

Shiina N, Tsukita S (1999) Mutations at phosphorylation sites of *Xenopus* microtubule-associated protein 4 affect its microtubule-binding ability and chromosome movement during mitosis. Mol Biol Cell 10:597–608.

Shiina N, Moriguchi T, Ohta K, Gotoh Y, Nishida E (1992) Regulation of a major microtubule-associated protein by MPF and MAP kinase. EMBO J 11:3977–3984.

Shiina N, Gotoh Y, Kubomura N, Iwamatsu A, Nishida E (1994) Microtubule severing by elongation factor 1α. Science 266:282–285.

Sigrist SJ, Thiel PR, Reiff DF, Lachance PED, Lasko P, Schuster CM (2000) Postsynaptic translation affects the efficacy and morphology of neuromuscular junctions. Nature 405:1062–1065.

Smart FM, Edelman GM, Vanderklish PW (2003) BDNF induces translocation of initiation factor 4E to mRNA granules: Evidence for a role of synaptic microfilaments and integrins. Proc Natl Acad Sci USA 100:14403–14408.

Stage-Zimmermann T, Schmidt U, Silver PA (2000) Factors affecting nuclear export of the 60S ribosomal subunit *in vivo*. Mol Biol Cell 11:3777–3789.

Steward O, Levy WB (1982) Preferential localization of polyribosomes under the base of dendritic spines in granule cells of the dentate gyrus. J Neurosci 2:284–291.

Steward O, Schuman EM (2001) Protein synthesis at synaptic sites on dendrites. Annu Rev Neurosci 24:299–325.

St Johnston D (1995) The intracellular localization of messenger RNAs. Cell 81:161–170.

Stukenberg PT, Lustig KD, McGarry TJ, King RW, Kuang J, Kirschner MW (1997) Systematic identification of mitotic phosphoproteins. Curr Biol 7:338–348.

Takei N, Kawamura M, Hara K, Yonezawa K, Nawa H (2001) Brain-derived neurotrophic factor enhances neuronal translation by activating multiple initiation processes. J Biol Chem 276:42818–42825.

Tang SJ, Meulemans D, Vazquez L, Colaco N, Schuman E (2001) A role for rat homolog of staufen in the transport of RNA to neuronal dendrites. Neuron 32:463–475.

Tang SJ, Reis G, Kang H, Gingras A-C, Sonenberg N, Schuman EM (2002) A rapamycin-sensitive signaling pathway contributes to long-term synaptic plasticity in the hippocampus. Proc Natl Acad Sci USA 99:467–472.

Tiedge H, Bloom FE, Richter D (1999) RNA, whither goest thou? Science 283:186–187.

Tongiorgi E, Righi M, Cattaneo A (1997) Activity-dependent dendritic targeting of BDNF and TrkB mRNAs in hippocampal neurons. J Neurosci 17:9492–9505.

Wilsch-Brauninger M, Schwarz H, Nusslein-Volhard C (1997) A sponge-like structure involved in the association and transport of maternal products during *Drosophila* oogenesis. J Cell Biol 139:817–829.

Wolffe AP (1994) Structural and functional properties of the evolutionary ancient Y-box family of nucleic acid binding proteins. BioEssays 16:245–251.

Yoshimori T, Yamagata F, Yamamoto A, Mizushima N, Kabeya Y, Nara A, Miwako I, Ohashi M, Ohsumi M, Ohsumi Y (2000) The mouse SKD1, a homologue of yeast Vps4p, is required for normal endosomal trafficking and morphology in mammalian cells. Mol Biol Cell 11:747–763.